Structures 66 (2024) 106895

Contents lists available at ScienceDirect

Structures

journal homepage: www.elsevier.com/locate/structures

Bending test of long-span ultra-shallow floor beam (USFB) with two lightweight concretes

Konstantinos Daniel Tsavdaridis [a,b,*], Brett McKinley [c], Burcu Nerkis Kacaroglu [a], Dan-Adrian Corfar [a], R. Mark Lawson [d]

[a] Department of Engineering, School of Science & Technology, Northampton Square, City, University of London, EC1V 0HB London, UK
[b] International Advanced Science and Technology Research Organization (IROAST), Kumamoto University, Kurokami, Kumamoto 8608555, Japan
[c] School of Engineering & Computing, University of Central Lancashire, PR1 2HE Preston, UK
[d] The Steel Construction Institute, Silwood Park, SL5 7QN Ascot, UK

ARTICLE INFO

Keywords:
Composite beams
Lightweight concrete slab
Ultra-shallow flooring system
Flexural test
Ultra-lightweight concrete
Flooring system

ABSTRACT

This paper presents the bending behaviour of a partially encased ultra-shallow floor beam (USFB) with two types of lightweight concrete. The beam was fabricated by welding two asymmetric Tees together along the web to create a beam with multiple circular openings that act as 'plug shear connectors' with the concrete encasement. The bending resistance of the plug-shear connection system was obtained by testing a composite USFB for a beam span of 7.2 m, half of the span being made with a lightweight concrete slab and the other half span with an ultra-lightweight concrete slab. Analysis of the four-point bending tests was carried out to determine the increase in bending resistance due to composite action and the contribution of the longitudinal shear connection due to the concrete plug passing through the web openings combined with additional tie bars. Calculations of the properties of the USFB with the two types of lightweight concrete were made according to SCI documentation and Eurocode 4. It was observed that the deflections were predicted accurately by the elastic properties and that the failure mode was by concrete crushing before the plastic bending resistance of the composite section had been developed. It was also shown that the cracked section properties should be used for the deflection analysis.

1. Introduction

Steel-concrete composite structural systems have been a subject of considerable research in the construction industry due to their efficiency in material utilisation and robust structural behaviour. Furthermore, reducing the depth of composite floors by use of slim floor construction allows more floors to be built when building heights are restricted or to insert new floors in existing buildings with height limitations [1,2].

Slim floor beams are used in residential buildings, in building extensions, in car parks and in basements, where asymmetric steel beams act compositely with the concrete encasement and so achieve the minimum structural depth with sufficient stiffness to satisfy serviceability limits of deflection and control of vibrations, which are generally the controlling criteria. Slim floor beams have an efficient span-to-depth ratio of 24 to 30 and there is an added advantage of using lightweight concrete to limit their self-weight deflection but without compromising the deflection under imposed loads due to composite action. Lightweight concrete is also considered strongly where loads on foundations have to be carefully controlled, for example in renovation projects.

In 2006, the Ultra Shallow Floor Beam (USFB) was developed, which is fabricated by welding two highly asymmetric Tees together along the web. These beams have a series of circular web openings along their length. Generally, the top Tee is cut from the Universal Beam (UB) or IPE section; and the bottom Tee is cut from a Universal Column (UC) or HE section. As a result, the beam's weight is reduced [19]. In the USFB manufacturing process, the diameter of the openings is linked to the beam depth. The steel beam is also required to support the loads during construction which means that the pure shear resistance of the perforated web is important.

Composite action is developed by the concrete passing through the circular web openings by bearing of the concrete on the beam web, which are known as 'shear plugs'. This form of shear connection can be enhanced by tie bars placed through alternate openings which act in shear as well as transverse reinforcement for robustness and fire resistance of the USFB [5,15]. The increased composite stiffness for vibration performance was also investigated [20,21].

* Correspondence to: Professor of Structural Engineering City, University of London.
E-mail address: konstantinos.tsavdaridis@city.ac.uk (K.D. Tsavdaridis).

https://doi.org/10.1016/j.istruc.2024.106895
Received 8 February 2024; Received in revised form 30 May 2024; Accepted 6 July 2024
Available online 13 July 2024

The context of the research presented in this current paper is to:

- Investigate the structural performance of a typical long span USFB with lightweight concrete and its composite action at the serviceability and ultimate limit states.
- Compare the test serviceability performance with predictions using the calculated elastic section properties of the composite USFB taking account of the elastic moduli of lightweight concretes and the potential for loss of stiffness due to end slip.
- Compare the test failure moment to the plastic bending resistance of the composite USFB calculated to EN 1994-1-1. Based on the test behaviour, identify if the concrete strength is reduced at the high compressive strains required to develop the plastic bending resistance of the composite section taking account of the position of the plastic neutral axis depth.
- Using the principles of partial shear connection, back-analyse the longitudinal shear forces developed by the shear plugs and tie reinforcement at the bending resistance in the test.

2. Background research on composite slim floor beams

Slim floor construction has been the subject of considerable research in recent years to determine the mechanism of composite action with concrete encasement and tie reinforcement, but no research has been carried out on the influence of the use of lightweight concrete on composite action, which is the subject of this paper. The use of lightweight concrete may be a good alternative for slim floors to further reduce the weight of the slabs and it may be efficiently used in plug shear systems capitalising on the partial concrete encasement. The following researchers focused on the critical behavioural aspects of the USFBs. Wang et al. [22] investigated the behaviour of two 'slim frame' beams with different reinforcement ratios. This showed that the effect of the reinforcement did not affect the elastic behaviour at serviceability, but it did affect the bending resistance in the tests.

Huo and D'Mello [12] performed push-out tests on short columns with 3 circular openings of 150 mm and 200 mm diameter using normal weight concrete between the flanges of the column to represent the shear connection in a composite USFB beam. Various forms of shear connection systems were tested including unreinforced plugs in the two concrete grades, 12 mm and 16 mm diameter tie bars and circular steel ducting through the openings. However, this research showed that the push-out test shear resistances are considerably higher than the longitudinal shear resistances back-analysed from beam tests, which shows that the plugs act differently in a flexural test on a beam than in a push-out test. Huo and D'Mello [13] also presented results of a 4-point bending test on a 230 mm deep composite USFB of 6 m span, similar to the one of the studies presented herein, using normal weight concrete in which one shear span had 16 mm diameter tie bars through alternate 150 mm diameter web openings and the other shear span relied on 9 unreinforced concrete plugs through the openings. The test bending resistance for the composite section was 50 % higher than the bending resistance of the steel USFB, and this moment corresponded to 46 % degree of shear connection on the side with unreinforced plugs. Bending failure occurred at an end slip of 6 mm which indicated that partial shear connection based on ductile shear connection had occurred. Back analysis of the longitudinal shear force gave a shear resistance of 50 kN per plug which is equivalent to a bearing stress of 37 N/mm^2 of the concrete on the steel web at the opening. This showed the good performance of concrete plugs as shear connectors in normal weight concrete.

More recently, Pereira Junior et al. [16] studied the flexural behaviour of USFBs with precast hollow-core slabs. It was concluded that steel tie bars passing through the web openings is important to composite action and the reinforcement of the concrete topping contributed to the crack control. Chen et al. [11] investigated partial shear connection in slim floor beams with circular openings combined with transverse reinforcement.

Sheehan et al. [17] presented the results of tests on 9 composite slim floor beams, most with reinforcing bars passing through small diameter web openings. The 6 m span beams used HEB20 sections with a 400 × 15 mm thick plate welded to the bottom flange. The total slab depth was 240 mm cast with formwork to form a 120 mm concrete topping and a 40 mm top cover to the beam with A252 mesh reinforcement over the beam. In one comparative test, the concrete was cast level with the top flange. Four tests were on beams with 16 mm diameter bars placed through 40 mm diameter web openings at 500 mm spacing, and one at 250 mm spacing and one at 1 m spacing. Further comparative tests had horizontally welded shear connectors and two had 80 mm diameter web openings. Most tests were subject to 2 load points at 1.5 m from the supports to create constant shear and moment zones and one test was carried out with simulated uniform loading applied at a 300 mm eccentricity to the beam axis to investigate the clamping action of the negative moment on the shear connection. The calculated degree of shear connection was 0%, 25 %, 40 %, and 100 % in the tests. All of the composite slim floor beams with bar reinforcement failed with considerable plastic deformation and end slips of 8 to 25 mm.

The Final EU Report [18] presents results of the project 'Slim App', which includes the beam tests Sheehan et al. [17] and push-out tests on the shear connection systems, serviceability tests on beams subject to long term loading and numerical investigations on strain compatibility in the highly asymmetric composite sections. A reduction factor on the plastic bending resistance is proposed based on the depth of the plastic neutral axis in the composite section and therefore, on the strain developed in the concrete.

3. Lightweight and ultra-lightweight concretes used in combination with USFB

Concrete with lightweight aggregates can achieve the compressive strength of normal weight concrete but with a lower density of 1300 to 1900 kg/m^3. Lightweight aggregate is typically pulverised fuel ash or expanded clay LECA [3,4].

Lytag aggregate has a bulk density of 700–800 kg/m^3 which is about half of the density of normal weight aggregates. Leca coarse and fine aggregates are used for ultra-lightweight concrete. Leca is manufactured from clay heated in a rotary kiln. A stiff outer shell and a porous interior give the clay grains their heterogeneous structure and the characteristic lightness during the manufacturing process. The bulk density of Leca aggregate is around 250–450 kg/m^3.

Brooks et al. [6] conducted mix design trials for lightweight structural concrete (LWC) with Lytag aggregate and ultra-lightweight structural concrete (ULWC) with Leca aggregate. LWC achieved 27.5 MPa strength with a 0.79 free water/cement ratio and a density of 1705 kg/m^3, while ULWC achieved 21 MPa with a 0.56 water/cement ratio and a density of 1295 kg/m^3.

The flexural behaviour of composite USFB is based on the concrete's strength and elastic modulus, which affect both the elastic and plastic bending properties and longitudinal shear connection, as noted by Tsavdaridis [19] in 2010. The aim of this study is to investigate the bending resistance and stiffness of an ultra-shallow flooring system using two different types of lightweight concretes, the LWC and ULWC presented by Brooks et al. [6].

The effect of the lightweight concrete on the shear resistance of the concrete 'plugs' combined with tie reinforcement is also an important parameter in this investigation. The test results are used to demonstrate the applicability of the existing design methodology for USFBs according to the Steel Construction Institute (SCI) guidelines and Eurocode 4. As for previous research on USFBs, a relatively long and shallow beam was used for testing to allow the shear connection mechanism to be fully developed and to compare the serviceability results with elastic theory.

3.1. Concrete mix details

In the USFB test, CEM I-52.5 R, 3.15 specific gravity (S.G) ordinary Portland cement was used for both types of concrete. The gradation of the used aggregates in comparison with the standard requirement for lightweight aggregates according to BS EN 13055 [9] is illustrated in Fig. 1.

Brooks et al. [6] studied three different mix designs for both types of concrete, lightweight (LWC) and ultra-lightweight (ULWC). The proportions of lightweight concrete mixes proposed by Brooks et al. are presented in Table 1.

LWC1 and ULWC1 mix designs were used in this study which had dry densities of 1295 kg/m^3 and 1705 kg/m^3 and compressive strengths of 21 N/mm^2 and 27.5 N/mm^2 at 28 days. Materials weights adopted from the Brooks study and used for the beam test are shown in Table 2.

Initial trial mixes were made for both types of concrete based on the material amounts given in Table 2. After being covered for 24 h, the fresh concrete cube and cylinder samples were moved into a wet room to cure. The compressive strength of lightweight concrete was found to be 33 MPa after 28 days, while that of ultra-lightweight concrete was 17 MPa. The slump value was 12 mm for the LWC and around 120 mm for the ULWC. Leca aggregates absorb water with time, so its slump value is higher than that of Lytag.

3.2. Concrete cube tests

Having established the suitability of the trial mixes, these mixes were used in the construction of the test beam. The concrete cube compressive strength was determined on the 7th, 28th, and 42nd day (one week before testing in accordance with BS EN 12390–3 [10] and Table 3 shows the cube results. In the LWC case, there was a noticeable gain of concrete strength after 28 days and its strength was more than twice that of the ULWC. It should be noted that the limiting strain of LWC concrete is about 2,500 micro-strain (0.0025) as can be seen in Fig. 2, which is less than the 0.0035 limiting strain of NWC. This shows that developing plastic stress blocks is more difficult for USFB with LWC, particularly where the plastic neutral axis is low in the composite section.

4. Bending tests on USFB beam

A four-point bending test was carried out to investigate the bending resistance and stiffness of the USFB with the lightweight and ultra-lightweight concrete (Fig. 3). The simply supported test beam had a zone of uniform bending and two zones of uniform shear. A solid slab was used to simplify the test construction and provide clarity of the influencing parameters, by ignoring the shape of the steel decking, for example. In the test, the slab depth was cast as equal to the beam depth and the solid concrete between the top and bottom flanges created the plug shear connection system. In practice, USFB with precast units or steel decking follows the construction details illustrated in Fig. 4 and would introduce other variables into the test.

The advantage of a 4-point bending test is that zones of uniform shear allow the longitudinal shear connection to be evaluated. But the disadvantage is that the load positions represent zones of high shear and moment, which might adversely affect the behaviour particularly where the shear resistance of the steel beam is reduced at the opening positions. But nevertheless, calculations showed that combined shear and bending effects at the load positions should not influence the failure mode

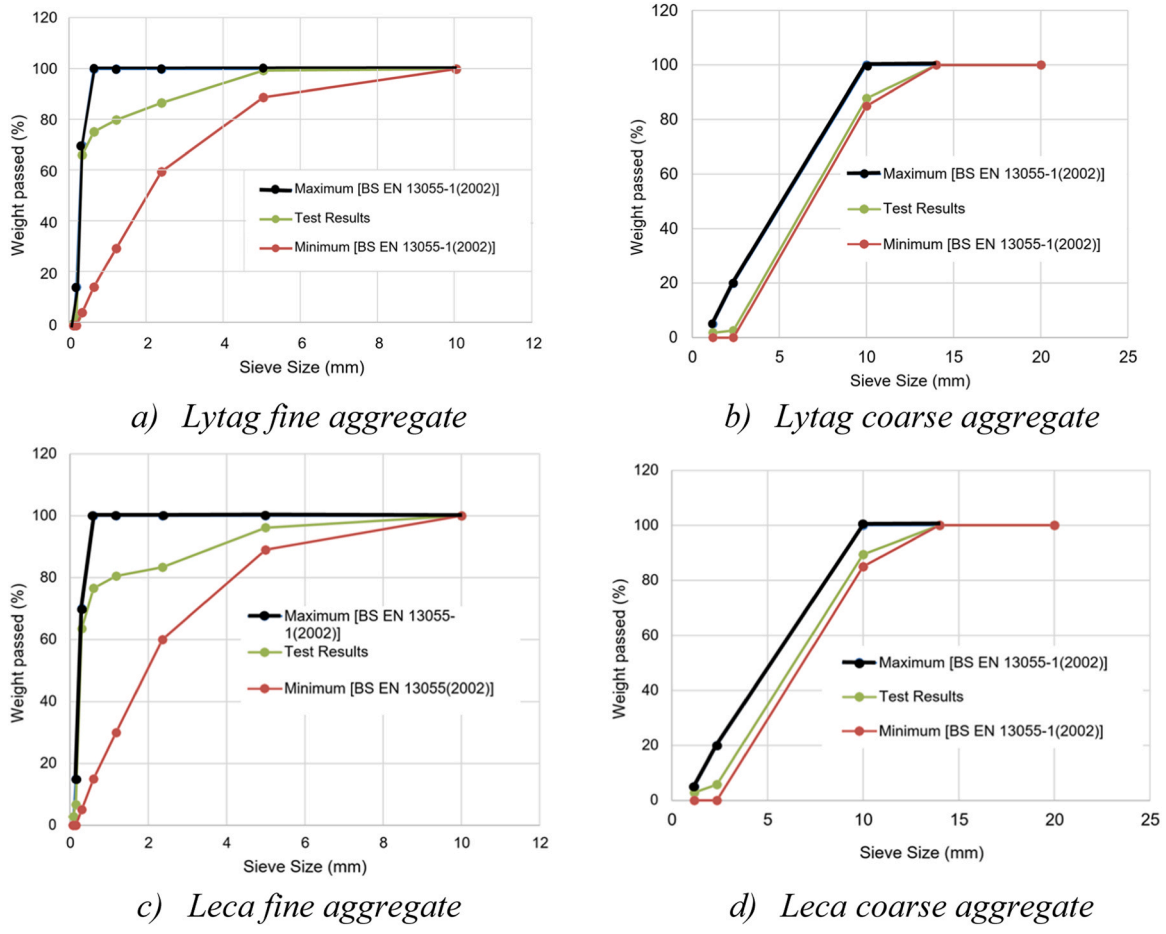

Fig. 1. Grading curves for lightweight aggregates.

Table 1
Material ratios and percentages for concrete mixture [6].

Concrete type	Aggregate type	Cement content (kg/m^3)	Aggregate /cement ratio	Fines (%)	Free water /cement ratio (%)	Absorption (%)	Compressive strength 28 days (MPa)
LWC 1	Lytag	250	4.58	54.6	0.79	9.8	27.5
LWC 2	Lytag	350	3.06	51.7	0.58	9.9	41.5
LWC 3	Lytag	452	2.23	48.2	0.46	9.9	52.5
ULWC 1	Leca	448	1.23	58.6	0.56	7.5	21
ULWC 2	Leca	349	1.75	62.6	0.71	7.6	18
ULWC 3	Leca	251	2.70	65.9	0.98	7.5	14

Table 2
Material weights for 1 m^3 concrete mixture.

Concrete type	Cement (kg/m^3)	Fine agg. (kg/m^3)	Coarse agg. (kg/m^3)	Free water (kg/m^3)	Absorbed water (kg/m^3)	Plastic density (kg/m^3)
LWC	250	625	520	197.5	112	1704.5
ULWC	448	323	228	251	41.3	1291.3

Table 3
Concrete properties.

Testing day	LWC Cube Compressive Strength, f_{cu}	ULWC Cube Compressive Strength, f_{cu}
7-day	21 N/mm^2	14 N/mm^2
28-day	28 N/mm^2	15.5 N/mm^2
42-day	38 N/mm^2	17.5 N/mm^2

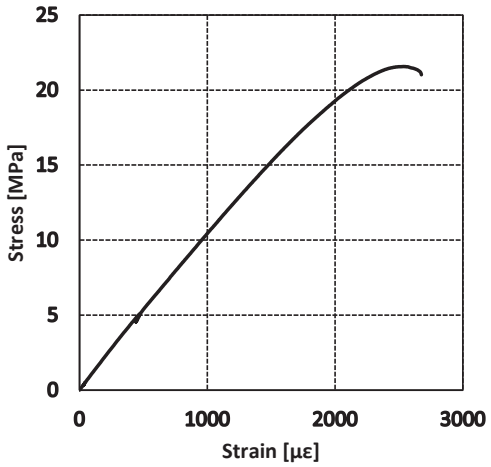

Fig. 2. Typical stress-strain graph for LWC (result at 7 days).

adversely and would not affect serviceability.

It was decided to develop the test on one USFB beam with the two lightweight concrete types all at once in order to eliminate the variability of the steel beam dimensions and strength, so that the difference between the two concretes could be shown. It was considered that the ULWC side would fail first and so loading the jacks equally on both sides would give a reliable result for the bending resistance for this side. Then, the jack loads could both be reduced and the jack on the LWC side could be loaded on its own to fail this side without further damaging the ULWC side. The loads and hence the applied moments could be interpreted by use of load cells. In practice during the test, although concrete crushing occurred first on the ULWC side, there was evidence of longitudinal slip on the LWC side and therefore the continued loading on one jack was not required.

4.1. Steel section and concrete slab

The test beam was 7.6 m long overall, but 100 mm of the section from both ends was not encased by concrete (see Fig. 5). The composite test beam's length was 7.4 m, and the span between supports was 7.2 m. The steel section was created by welding a top Tee section taken from a 305 × 127 × 37 UB and a bottom Tee section taken from a 254 × 254 × 73 UC (asymmetry ratio of flange areas of approximately 2). The steel was grade S355JR and the cellular beam had an overall depth of 210 mm. The beam had 25 regular circular web openings of 100 mm diameter at 300 mm spacing along the beam. Data for the USFB steel beam and the final composite beam are given in Table 4. The span-to-depth ratio was 34, which is at the upper limit of the practical use of USFB.

The slab width was 1.0 m, which was less than the 1.8 m (span/4) effective width recommended by Eurocode 4 [7]. This was done to avoid overestimating the composite action that could be developed. The top and bottom flanges of the beam were cast level with the surfaces of the concrete, which was therefore 210 mm deep.

A 16 mm tie-bar of 1.0 m length was placed in the middle of alternate openings. Lightweight concrete (LWC) was used for half of the span, and ultra-lightweight concrete (ULWC) was used for the other half of the span. This type of dual testing was also implemented in the literature [13] and it serves two purposes; testing under the exact same laboratory ambient conditions the steel-concrete composite beam specimen and reducing the amount of material used for casting. Since the concretes were required in relatively large quantities, the LWC side was cast first, and then the ULWC side was cast on the next day. The mixer (Teka Mix Turbine) has a microwave-based moisture measurement built into it. Once the first batch was mixed and found acceptable via a slump test, the moisture measurement was used to mix all subsequent batches, thus ensuring uniformity (i.e., it compensates for any variation of moisture content in the aggregates).

All the specimens had the same curing conditions, and the composite beam was covered with plastic sheets as shown in Fig. 6.

4.2. Test setup and instrumentation

Fig. 7 shows the configuration for the four-point bending test. The reaction beam was supported by two additional beams to connect to pairs of Macalloy bars passing through the reaction floor. Two 100 kN (10 tonnes) hydraulic jacks were attached to the reaction beam. The bottom flange of the USFB and concrete slab were in contact with rollers at the supports.

At mid-span and at the loading points, potentiometers were used to measure the beam deflections, as shown in Fig. 7c, while the slips between the steel section and concrete slab were measured using horizontal potentiometers mounted at the end supports. The potentiometers measuring vertical displacement (PO1 – PO3) were attached to an independent and free-standing frame not affected by any loading thereby ensuring displacements recorded are not influenced by elasticity of the loading frame. Transducers PO4 and PO5 measuring horizontal slip were attached directly to the steel beam and measured to the concrete face, thereby directly measuring slip without a need to perform any secondary calculations.

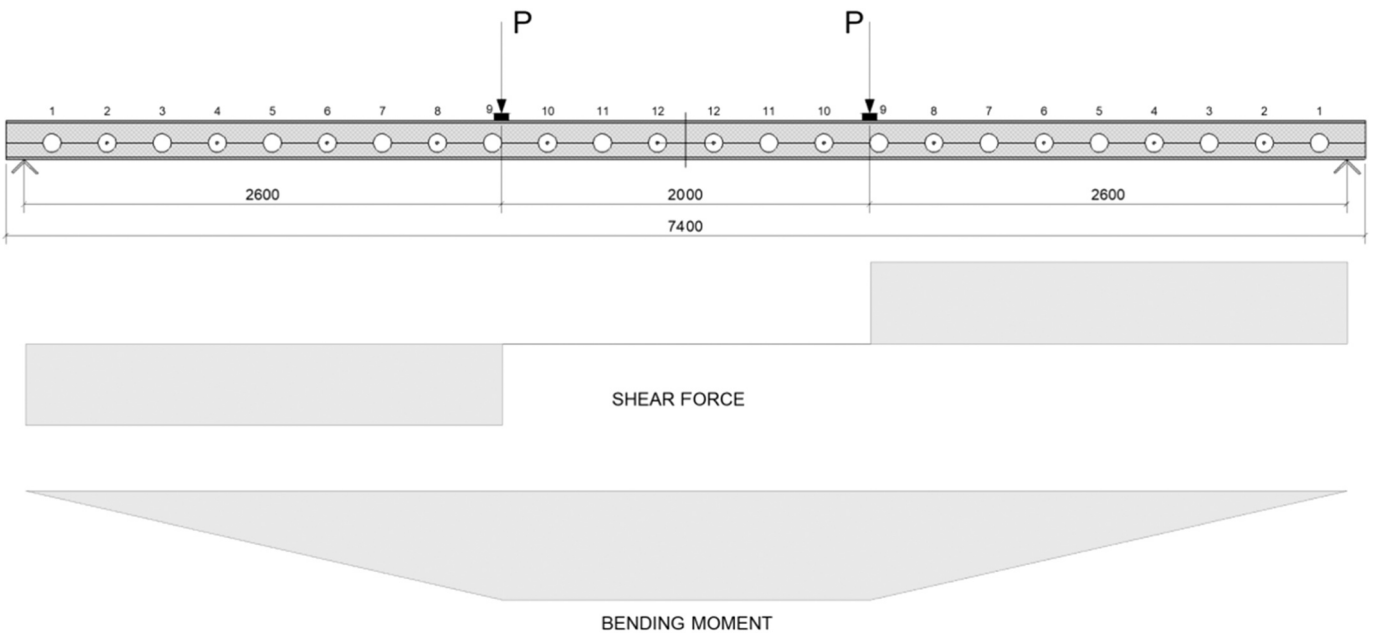

Fig. 3. Four-point bending test loading arrangements, shear force and moment diagrams.

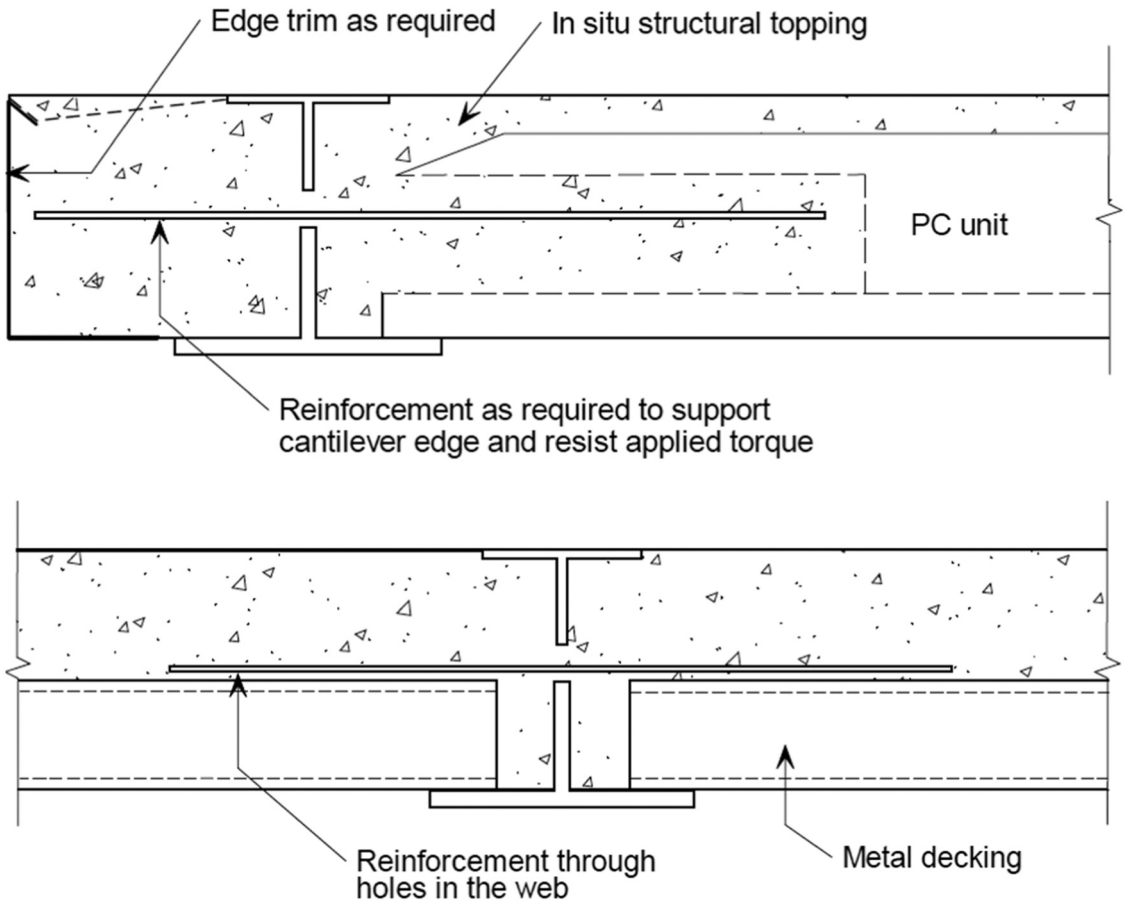

Fig. 4. Typical construction details of USFB with precast concrete units or steel decking [14].

4.3. Testing procedure

The four-point bending test was devised to give the required ratio of bending moment to shear force to be able to fail the composite USFB either in pure bending or longitudinal shear connection, The potential failure modes are:

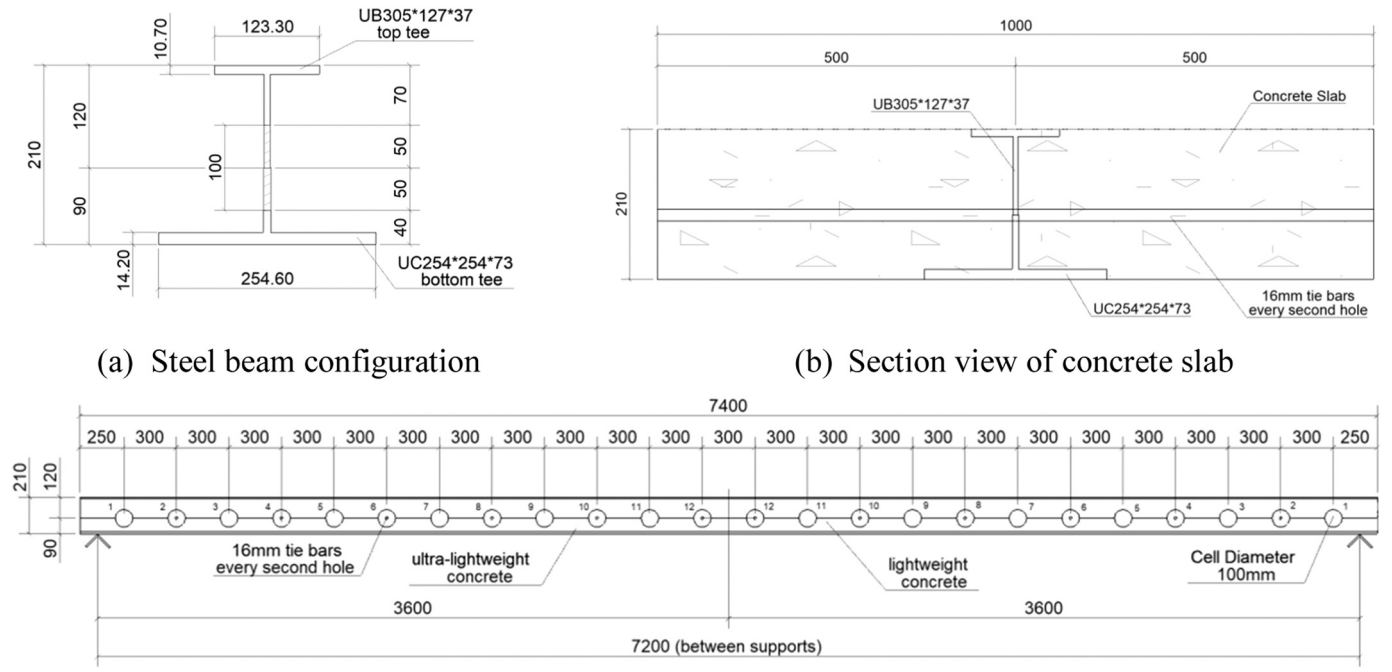

Fig. 5. Details of the fabricated USFB (all dimensions in mm).

Table 4
Summary of USFB beam data.

Slab depth × width	Beam and Openings	Tees cut from	Depth of Tee	Flange thickness	Web thickness	Area of Tee	Tee neutral axis depth*	Properties of steel USFB at openings
210 mm deep × 1 m width	210 mm deep beam with 100 mm dia. openings at 300 mm centres	305 × 127 × 37 kg/m UB	70 mm	10.7 mm	7.1 mm	1740 mm^2	8 mm	Inertia 43.1×10^3 mm^4
		254 × 254 × 73 kg/m UC	40 mm	14.2 mm	8.6 mm	3837 mm^2	8 mm	Neutral axis depth $z_e = 143$ mm

*measured from outside of flange

- Pure flexural failure by yielding in the steel section so that the composite section develops its plastic bending resistance.
- Crushing of the LWC or ULWC crushing before the plastic bending resistance of the composite section is developed.
- Longitudinal shear failure of the reinforced shear plugs through the openings before the plastic bending resistance of the composite section is developed.
- Pure shear failure of the perforated web of the USFB at the centreline of the openings.
- *Vierendeel* bending of the perforated steel section subject to shear.

The test beam span-to-depth ratio of 34 suggests that flexure or concrete crushing rather than shear would be the dominant mode of failure at large deflections. Calculations of the shear and bending resistances before testing were made and are presented later in the paper. The test USFB beam was cast on the strong floor and so the self-weight load after lifting into position was applied to the composite section. It is also necessary to check the deflection of the composite section at serviceability, which will often be the controlling case for slim floor beams. Therefore, the increase in the inertia due to composite action of the lightweight concretes with the USFB section is an important parameter that was obtained from the test results and compared to the theoretical resistance.

During the test, load was applied equally to both jacks using a manually controlled, electrically powered hydraulic pump with a flow control valve fitted to the pump outlet throttling the rate of oil flow (a form of displacement control) until the desired load or deflection had been reached. At the peak load or displacement for each increment, the oil flow (hence displacement) was held static for a period before being reversed to unload the beam and record any residual and permanent deflection. Subsequent cycles were repeated with increasing peak load until the beam exhibited a peak load response and the onset of plasticity, at which point the deflections were increased until failure by one of the aforementioned mechanisms was identified.

The proposed test plan called for the first cycle to load until 50 % of the expected peak load, with subsequent cycles increasing or repeating (to determine any hysteresis) to 100 % of the expected load. A final cycle was then used to find the maximum peak load before increasing displacements until failure by one of the mechanisms listed above.

5. Beam test results

5.1. Load-deflection curves

A summary of the test data corresponding to the 7th load (failure) cycle is given in Table 5. More detailed data of each loading cycle and corresponding deflections as well as residual deflections after release of the load are presented in Table 6. Jack loads and deflections for the two sides of the beam for selected load cycles is summarised in Table 7.

The composite USFB essentially behaves elastically up to close to the failure load of 88 kN per jack on the 7th cycle of load which shows that plasticity of the steel section has not developed (Fig. 8). Also, no local

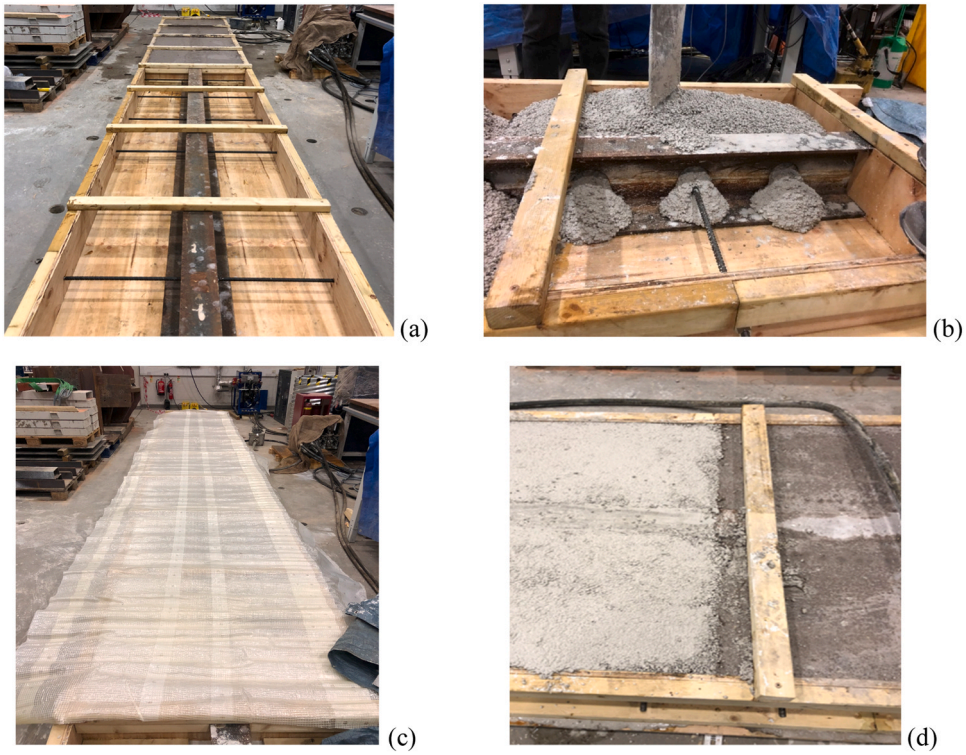

Fig. 6. Casting and curing of the USFB specimen.

buckling of the top flange of the USFB occurred. The back-analysis of the test (Appendix) showed that the limiting condition is crushing of the concrete in both types of lightweight concrete. The test showed that crushing of the ULWC occurred at mid-span at the junction of the two types of concrete (Fig. 10c).

Up to the failure point, the test showed that elastic behaviour applies. The composite stiffness was calculated from the cracked section properties by determining the depth of concrete in compression assuming that the concrete in tension has no stiffness and using the ratio of the elastic moduli of steel to concrete for the two types of concrete in compression. The calculated composite stiffness of the composite USFB section for the two types of concrete is 1.89 and 1.55 times the stiffness of the steel USFB beam. The average composite stiffness used to calculate the mid-span deflection agrees well with the measured deflection up to the failure load of 88 kN.

On the 8th cycle of load, end slip was observed (Fig. 9b) with a loss of some of the composite stiffness, and the maximum jack load reached on this cycle reduced to 83 kN. Back-analysis of the longitudinal shear force in the four reinforced plugs at the openings showed that the test longitudinal force exceeded the shear resistance of the 16 mm diameter bars at the 4 plugs. This implies that additional longitudinal shear resistance was achieved by bearing of the lightweight concrete on the edge of all of the openings, validating outcomes from studies found in the literature. Back-analysis of both concrete types suggests that the local bearing strength of the concrete on the beam web was approximately 2 times the concrete cube strength.

No evidence of pure shear failure or *Vierendeel* bending failure of the USFB at the openings was observed, which was in good agreement with the analytical prediction using Eqs. (10)-(12) in the Appendix. Therefore, the dominant modes of failure are concrete crushing at the elastic limiting strain of the two concrete types (Fig. 10) and longitudinal shear failure of the reinforced plugs, which occurred at a similar load. The calculated plastic bending resistance of the steel USFB section using the measured steel strength is 132 kNm (Eqs. (8) and (9) in the Appendix) and so the test bending resistance of the composite section was 1.91 times the bending resistance of the steel USFB section, which shows good composite action.

5.2. Crack patterns

Vertical flexural cracks were observed during the test to indicate flexural cracking of the concrete. Diagonal cracks were not seen at any stage of the loading. Cracks started to occur at different times for the two types of concrete. Due to the lower strength of Leca-ULWC concrete, cracks occurred in the early loading stage. After the loading of 10 kN on each hydraulic jack (11 % of the failure load), the first cracks appeared near mid-span on the lower part of the concrete and propagated through approximately 60 % of the beam height in the following loading stages. Cracks appeared to be evenly spaced along the constant moment area at approximately 200 mm apart. Fig. 11a shows the cracks in the Leca-ULWC concrete part of the beam.

The Lytag-LWC concrete showed less noticeable cracking due to its higher strength characteristics, and flexural cracks became apparent about 50 % of the maximum test load. First cracks were initially thin and short in length. These cracks propagated upward to about half of the concrete depth at the later loading stages. In addition, cracks in the USFB with the LWC are shown in Fig. 11b.

6. Analysis of the beam test based on elastic and plastic principles

The elastic and plastic behaviours of the composite USFB are shown in Fig. 12. For elastic design, a linear strain variation through the cross-section is used with no discontinuity due to interface slip and the concrete in tension is assumed to be cracked and ineffective. The position of the elastic neutral axis is determined by the modular ratio, n, which is the ratio of the elastic moduli of steel to concrete and the asymmetry of the steel section.

Plastic design applies at high strains in the steel and concrete, so that plastic stress blocks are developed. The plastic neutral axis position is dependent by equating the concrete force and the compression resistance of the top Tee to the tension resistance of the bottom Tee. In cases

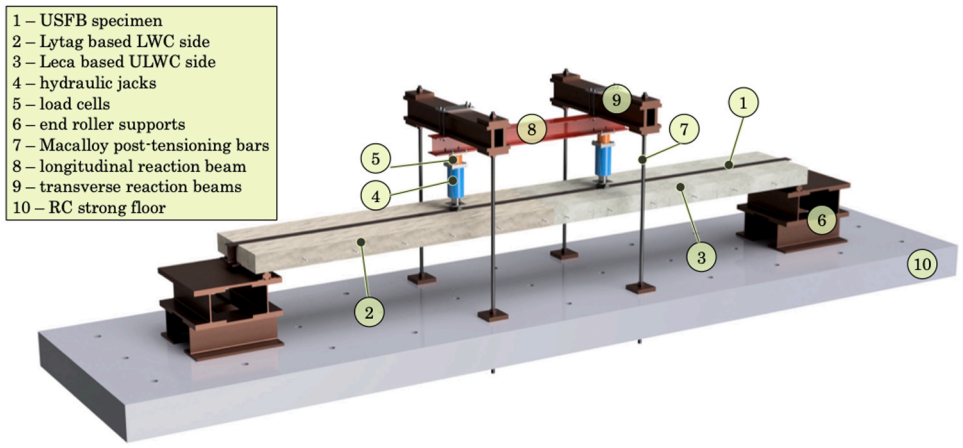

(a) Schematic of the USFB and its loading system

(b) View of the test frame showing the junction of the two types of concrete

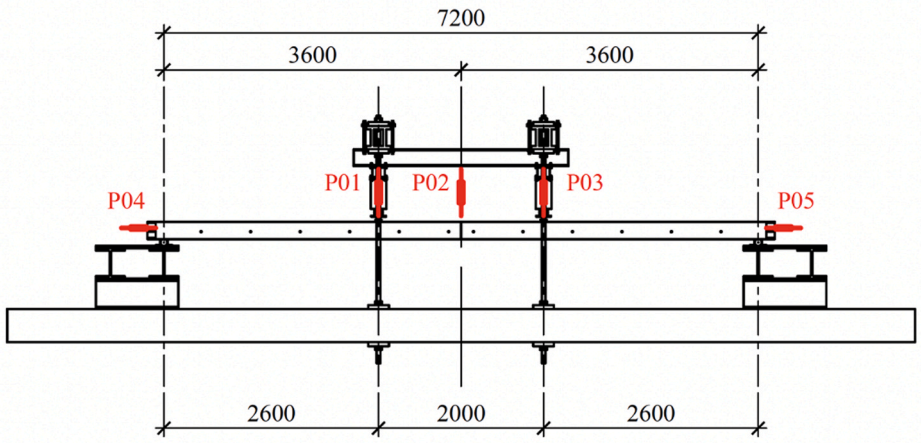

(c) Overall test frame dimensions and potentiometer layout

Fig. 7. Setup details of the four-point bending test.

Table 5
Summary of test results for the 7th load cycle.

Failure load per jack	Additional shear from self-weight	Total shear force at failure, V_{test}	Moment from jack load	Additional moment from self-weight	Total moment at failure, M_{test}
88 kN	13 kN	101 kN	229 kNm	23 kNm	252 kNm

of high asymmetry, the plastic neutral axis may lie in the lower part of the steel section, which implies that high strains are developed in the concrete and in the top flange.

The analysis of the composite properties of the two sides of the beam are given in Table 4.

6.1. Elastic bending resistance of composite USFB with LWC

The elastic bending resistance of the cracked section is obtained from

Table 6
Loading cycles, applied loads and deflections.

Loading cycle	Peak load	Peak deflection			Residual deflection after unloading		
		ULWC side	Mid-span	LWC side	ULWC side	Mid-span	LWC side
1st	46 kN	38 mm	40 mm	37 mm	2.5 mm	2.9 mm	2.6 mm
2nd	78 kN	66 mm	70 mm	65 mm	4.3 mm	4.7 mm	4.3 mm
3rd	70 kN	61 mm	64 mm	60 mm	4.1 mm	5.0 mm	4.2 mm
4th	88 kN	80 mm	84 mm	78 mm	7.6 mm	8.7 mm	7.7 mm
5th	82 kN	76 mm	81 mm	75 mm	7.5 mm	8.6 mm	7.7 mm
6th	80 kN	74 mm	79 mm	73 mm	7.7 mm	8.9 mm	8.0 mm
7th	88 kN	83 mm	89 mm	82 mm	9.6 mm	11.2 mm	9.7 mm
8th	83 kN	140 mm	186 mm	154 mm	60 mm	102 mm	82 mm

Table 7
Summary of jack loads and deflections for the two sides of the beam for selected load cycles.

Cycle no.	Deflection at P1 ULWC side	Deflection at P2 LWC side	Jack load P1	Jack load P2	Moment M1 at ULWC side	Moment M2 at LWC side
1	38 mm	37 mm	46 kN	46 kN	120 kNm	120 kNm
2	66 mm	65 mm	79 kN	77 kN	203 kNm	202 kNm
4	79 mm	78 mm	89 kN	87 kN	229 kNm	228 kNm
7 Failure	83 mm	82 mm	90 kN	87 kN	231 kNm	229 kNm
8 Post-failure			87 kN	82 kN	222 kNm	218 kNm

Note: Additional moment at jack positions due to beam self-weight is 22 kNm on LWC side and 21 kNm on ULWC side.

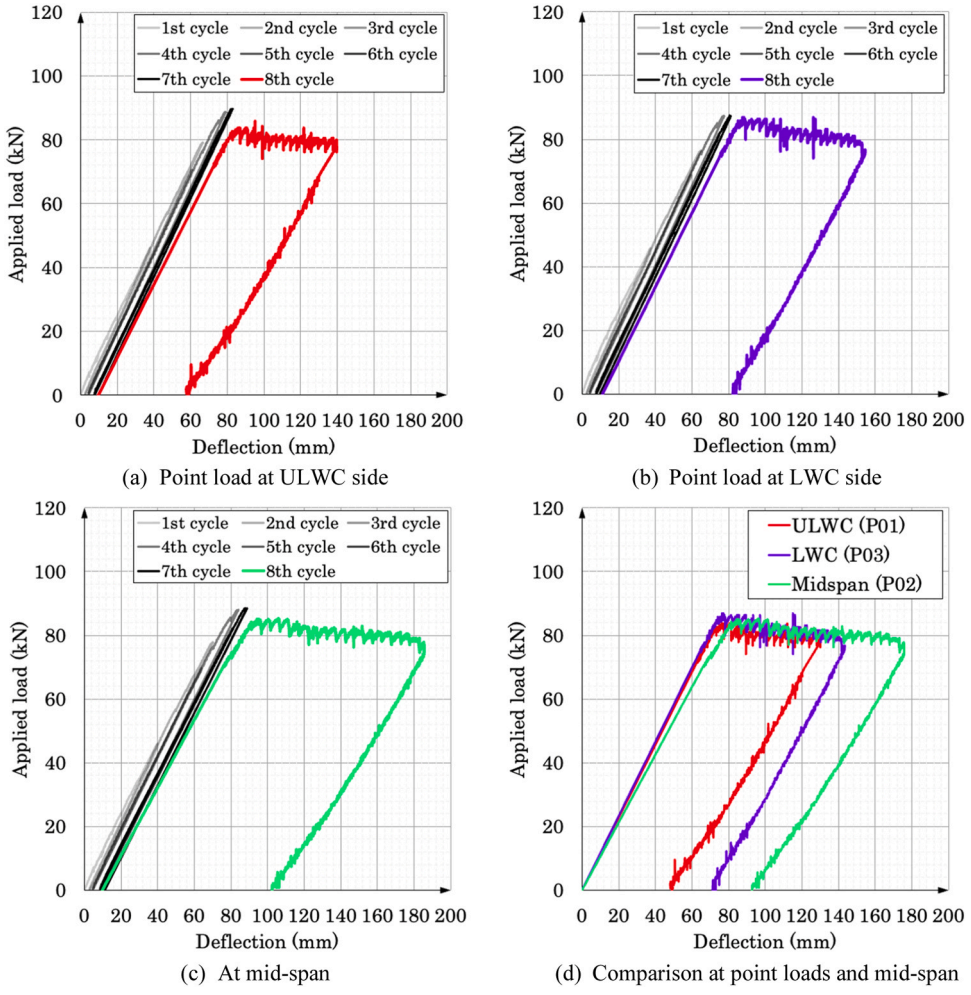

(a) Point load at ULWC side
(b) Point load at LWC side
(c) At mid-span
(d) Comparison at point loads and mid-span

Fig. 8. Load-displacement curves for the USFB test.

(a) No significant end slip during first 7 cycles

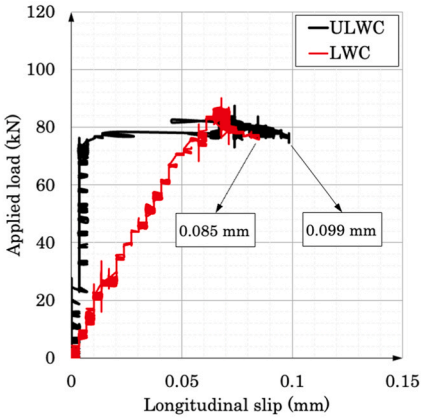

(b) End slip recorded during 8th cycle

Fig. 9. Load-slip behaviour of the USFB test.

(a) Deformed shape of the USFB during the 8th load cycle

(b) Initiation of wide cracks at the underside of the deformed USFB during the 8th cycle

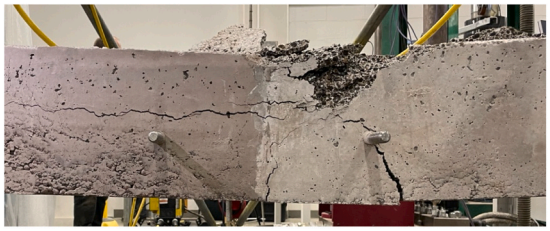

(c) Concrete crushing at mid-span of the USFB after the test

(d) Residual deflection of the USFB after the test

Fig. 10. Failure modes of the composite USFB.

(a) ULWC side of the beam (b) LWC side of the beam

Fig. 11. Concrete crack development.

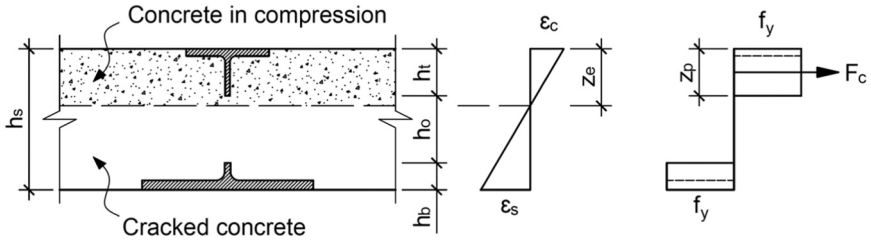

Fig. 12. Elastic strains and plastic stress blocks in the composite USFB section.

equilibrium of the compression and tension forces in the cross-section assuming that concrete only acts in compression over its neutral axis depth, z_e. The elastic neutral axis depth is determined from the quadratic equation given in expression (1):

$$z_e^2 + 2z_e\frac{n(A_b + A_t)}{b_c} - 2\frac{n(A_b(h_s - z_b) + A_t z_t)}{b_c} = 0 \quad (1)$$

Where $n = E_s/E_c$.

A_b = cross-sectional area of bottom Tee.

A_t = cross-sectional area of top Tee.

b_c = width of slab.

E_c=elastic modulus of concrete.

E_s =elastic modulus of steel.

h_s = depth of beam.

z_b= neutral axis position of bottom Tee from outside of section.

z_e= neutral axis position of composite section from top of section.

z_t = neutral axis position of top Tee from outside of section.

For the LWC side, this calculation using the test data shows that z_e is equal to 84 mm measured from the top of the slab.

For a compression strain ε_c at the top of the section, the bending resistance of the composite section is given by Eq. (2):

$$M_{comp.el} = \frac{z_e^2 b_c}{3}E_c\varepsilon_c + \frac{(z_e - z_t)^2}{z_e}A_t E_s\varepsilon_c + \frac{(h_s - z_e - z_b)^2}{z_e}A_b E_s\varepsilon_c \quad (2)$$

For the LWC side, the elastic bending resistance (in kNm), $M_{comp.el}$, for $z_e = 84$ mm is equal to $198.6 \times 10^3 \times \varepsilon_c$.

The inertia of the composite section, I_{comp}, is (in steel units) given by expression (3):

$$I_{comp} = \frac{M_{comp.el}z_e}{E_s\varepsilon_c} = 198.6 \times 10^6 \times \frac{84}{210} = 79.4 \times 10^6 \quad mm^4 \quad (3)$$

This is 1.84 times the inertia of the steel USFB.

For $M_{comp,el} = M_{test} = 252$ kNm at failure (Table 5), the strain in the concrete, ε_c, is equal to 1269×10^{-6} from Eq. (3). This strain is equal to an elastic stress in the LWC of $\sigma_c = E_c \times \varepsilon_c = 18.7 \times 10^3 \times 1269 \times 10^{-6} = 23.7$ N/mm^2. This may be compared to a design concrete strength of $0.67 \times 38 = 25.4$ N/mm^2 (with a partial factor of 1.0) which shows that the limiting condition may be the compression stress in the concrete at the elastic bending resistance of the composite section.

The strain in the bottom Tee, ε_s, is determined as shown in expression (4):

$$\varepsilon_s = \varepsilon_c \frac{(h_s - z_e - z_b)}{z_e} = 1269 \times 10^{-6} \times \frac{118}{84} = 1783 \times 10^{-6} < \varepsilon_y = f_y \Big/ E_s = 1857 \times 10^{-6} \quad (4)$$

This shows that the yield strength of the bottom Tee is not developed at the elastic bending resistance of the composite section.

Longitudinal shear force of composite USFB with LWC.

The compression force in the concrete, F_c, for an elastic stress, σ_c, of 23.7 N/mm^2 is given by expression (5):

$$F_c = 0.5\sigma_c z_e = 0.5 \times 23.7 \times 84 \times 10^3 \times 10^{-6} = 995\text{kN} \quad (5)$$

For 4 reinforced shear plugs in the shear span, the shear force per plug is equal to 995/4 = 249 kN. The shear resistance, $F_{s.bar}$, of a 16 mm dia. reinforcing bar (f_y = 500 N/mm^2) is 70 kN for tie bars passing through the openings, and so the combined shear resistance is 2 $F_{s.bar}$ = 140 kN. It follows that the unreinforced plugs also add to the longitudinal shear resistance and each of the 9 plugs resist a shear force, F_{plug}, due to bearing of the LWC concrete on the beam web given by Eq. (6):

$$F_{plug} = (F_c - 4 \times 2 \times F_{s.bar})/9 = 48.3\text{kN} \quad (6)$$

For an average web thickness of 7.8 mm and 100 mm opening diameter, the plug bearing stress of the LWC on the beam web is 62 N/mm^2, which is approximately 1.6 times the concrete cube strength.

6.2. Elastic bending resistance of composite USFB with ULWC

The elastic analysis is repeated for the ULWC with its lower elastic modulus and hence higher modular ratio of steel to concrete. In this case, the elastic neutral axis depth, z_e, is calculated from Eq. (1) as 100 mm from the top of the section. From Eqs. (2) and (3), the inertia of the composite section is 69.5 × 10^3 mm^4, which is 1.61 times the inertia of the steel USFB and 87 % of the inertia of the composite section on the LWC side.

Hence, for $M_{compl,el}$ = 252 kNm at failure, the concrete strain, ε_c, is equal to 1725 × 10^{-6}. This strain is equal to an elastic stress in the ULWC of σ_c = 9.6 × 10^3 × 1725 × 10^{-6} = 16.5 N/mm^2. This may be compared to a design compression strength of 0.67 × 17.5 = 11.7 N/mm^2 and shows that the limiting condition is the concrete strain at the elastic bending resistance. Yielding does not occur in either Tee for the ULWC side of the beam.

Longitudinal shear force of composite USFB with ULWC.

The compression force in concrete, F_c, is calculated as 828 kN and the shear force per plug is equal to 828/4 = 207 kN. It follows that the unreinforced plugs each resist a longitudinal shear force, F_{plug}, due to bearing of the concrete on the beam web is equal to (828–4 ×140)/9 = 30 kN. The plug bearing stress of the ULWC on the beam web is calculated as 38.4 N/mm^2, which is approximately 2.2 times the concrete cube strength.

Based on these analyses, the elastic properties of the composite section for the two concrete types are presented in Table 8.

6.3. Deflection of composite beam

At a failure load, P = 88 kN, the elastic mid-span deflection for an average inertia, $I_{comp,av}$ = 74.4 × 10^6 mm^4 is calculated as per expression (7), where L was the total length of the USFB between the end supports and a was the distance from each jack load to the corresponding end support as seen in Fig. 7.

$$d = \frac{Pa}{24E_s I_{comp.av}}(3L^2 - 4a^2) = \frac{88 \times 2.6 \times 10^9}{24 \times 210 \times 74.4 \times 10^6} \times (3 \times 7.2^2 - 4 \times 2.6^2) = 78.4\text{mm} \quad (7)$$

This theoretical deflection may be compared to a measured deflection of 89 – 9 = 80 mm on the 7th cycle of load, which is in good agreement and shows that the behaviour is elastic up to the failure load and its behaviour may be predicted from the cracked section properties of the composite USFB section.

6.4. Plastic bending resistance of composite section

The plastic bending resistance of the composite USFB section was also calculated from the plastic stress blocks to BS EN 1994–1-1 using the measured concrete and steel strengths.

For plastic design of the LWC side of the beam, the calculated degree of shear connection is 78 % at the test failure moment of 252 kNm and for a steel USFB bending resistance of 132 kNm. This is equivalent to a longitudinal shear force in the concrete of 636 kN, which is 64 % of the force obtained from elastic design at the failure moment. However, plastic failure did not occur in the test on this side of the beam.

For plastic design of the ULWC side of the beam, the calculated degree of shear connection is 85 % at the test failure moment. This is equivalent to a longitudinal shear force of 704 kN, which is 85 % of the force obtained from elastic design. It was apparent from the test that concrete crushing on the ULWC side of the beam occurred in elastic conditions before the plastic bending resistance of the composite USFB could be developed.

It is also known that the depth of the plastic neutral axis in a composite slim floor beam affects the development of its plastic bending resistance [18] due to the limiting concrete strain. On the ULWC side of the beam, the plastic neutral axis depth from the top of the section is at approximately 35 % of the beam depth which would lead to a reduction of about 10 % in its plastic bending resistance for S355 steel according to this guidance.

This shows that plastic design for slim floor beams with lightweight concrete is not a sufficiently reliable method of design based on current limited test data.

7. Concluding remarks

This paper examines the flexural behaviour of an ultra-shallow floor beam (USFB) encased in two different types of lightweight concrete. The USFB section was created by welding two asymmetric Tees and the 100 mm diameter circular openings were filled with concrete to create plug shear connectors. Also, 16 mm diameter tie bars were placed in alternate openings to act as additional shear connectors. A four-point bending test was conducted on the 7.2 m span beam to determine the bending resistance and stiffness of the composite USFB. The results of the bending test led to the following conclusions:

Table 8
Summary of composite beam data based on elastic analysis at the failure moment.

USFB with:	Concrete properties		Inertia of composite section, mm^4 (steel units)	Depth of concrete in compression, z_e	Strain in top of concrete at failure	Stress in concrete at failure, N/mm^2	Longitudinal force in concrete at failure
	f_{cu} N/mm^2	E_c kN/mm^2					
LWC	38	18.7	79.4 × 10^6	84 mm	1269 × 10^{-6}	23.7	995 kN
ULWC	17.5	9.6	69.5 × 10^6	100 mm	1725 × 10^{-6}	16.5	828 kN

- Composite action of the test beam increased the bending resistance by 91 % compared to the USFB steel section for both types of lightweight concrete.
- The ultra-lightweight concrete made with Leca aggregate began to show cracks before the serviceability deflection limit of 20 mm (=span/360). This confirms that the cracked section properties should be used for the deflection analysis.
- The lightweight concrete made with Lytag aggregate started to show cracks after the serviceability deflection limit.
- The elastic properties of the composite beam using the cracked concrete section gave similar results to the test in terms of the calculated deflection.
- Failure occurred on the 7th load cycle with a maximum jack load of 88 kN. The residual deflection at mid-span after this load cycle was 11.2 mm.
- Failure occurred by concrete crushing on the ULWC side. The bending resistance could be predicted using the cracked elastic section properties limited by the measured concrete strength.
- The maximum load on the 8th load cycle was 83 kN which indicated that some loss of composite action had occurred. A small end slip was recorded at the ends of the beam on this load cycle which showed that the additional tie bars were effective in resisting longitudinal shear.
- The longitudinal shear force that is developed by composite action in the beam test can be resisted by the combination of the shear resistance of the two shear planes of the tie bars and the plug shear connectors for types of lightweight concrete.
- For these types of LWC, it is shown that the strain capacity of the concrete limits the development of the plastic bending resistance in the USFB section and it is concluded that elastic designs should be used, particularly for ULWC.
- If plastic design is used to interpret the tests, the corresponding degree of shear connection at failure was calculated to be about 80 % using measured material strengths.
- In conclusion, the use of the two types of light weight concrete is shown to be structurally acceptable and can be predicted by elastic design of the cracked composite section for full shear connection.

CRediT authorship contribution statement

Mark R Lawson: Writing – review & editing, Validation, Supervision, Investigation. **Brett McKinley:** Writing – review & editing, Validation, Supervision, Methodology, Data curation, Conceptualization. **Dan-Adrian Corfar:** Writing – review & editing, Visualization, Validation, Investigation. **Burcu Nerkis Kacaroglu:** Writing – original draft, Formal analysis, Data curation. **Konstantinos Daniel Tsavdaridis:** Writing – review & editing, Validation, Supervision, Resources, Project administration, Methodology, Investigation, Funding acquisition, Formal analysis, Data curation, Conceptualization.

Declaration of Competing Interest

The authors declare that they have no known competing financial interests or personal relationships that could have appeared to influence the work reported in this paper.

Appendix: General test data for composite USFB

Failure point load in test $P_{test} = 88$ kN.
Span of beam $L = 7.2$ m.
Load application position a = 2.6 m.
Bending moment $M_{jack} = P_{test}$ a = 229 kNm.
Self-weight of beam $W_{sw} = 3.6$ kN/m (average of both sides).
Additional bending moment $M_{sw} = W_{sw} L^2/8 = 23$ kNm at mid-span.
Total moment at failure $M_{test} = M_{jack} + M_{sw} = 252$ kNm.
Additional shear force, $V_{sw} = W_{sw} L/2 = 13$ kN.
Total shear force at failure $V_{test} = P_{test} + V_{sw} = 101$ kN.
Data for beam:
Depth of beam $h_s = 210$ mm.
Width of slab $b = 1000$ mm.
Area of top Tee $A_t = 1740$ mm^2.
Area of bottom Tee $A_b = 3837$ mm^2 ($= 2.2\ A_t$).
Measured steel strength $f_y = 390$ N/mm^2.
Inertia of steel USFB, $I_s = 43.1 \times 10^3$ mm^4.
Bending resistance of the steel beam:

$$M_{pl} = (h_s - z_t - z_b)A_t f_y = (210–2 \times 8) \times 1740 \times 390 \times 10^{-6} = 132\text{kNm} \tag{8}$$

Ratio of moment due to composite action with the concrete encasement to the steel bending resistance:

$$\frac{M_{test}}{M_{pl}} = \frac{252}{132} = 1.91 \tag{9}$$

Pure shear resistance of the Tees, where $A_{v.t}$ and are the shear areas of the top and bottom Tees, as in Eurocode 3, Part 1–1 [8].

$$V_{Rd} = V_{t.Rd} + V_{b.Rd} = A_{v.t}\frac{f_y}{\sqrt{3}} + A_{v.b}\frac{f_y}{\sqrt{3}} = 125 + 104 = 229\text{kN} > 101\text{kN} \tag{10}$$

This shows that the ratio of the shear force at failure to the shear resistance is 44 %.

The sum of the *Vierendeel* bending resistances at the four corners of the opening, where $M_{Vier,Rd,t}$ and $M_{Vier,Rd,b}$ are the bending resistances of the top and bottom Tee respectively:

$$M_{Vier.Rd} = 2M_{Vier.Rd.t} + 2M_{Vier.Rd.b} = 5.6 + 4.7 = 10.3\text{kNm} \tag{11}$$

Applied *Vierendeel* moment across opening:

$$M_{Vier,Ed} = 0.45 h_o V_{test} = 0.45 \times 100 \times 101 \times 10^{-3} = 4.5\text{kNm} < 10.3\text{kNm} \quad (12)$$

This shows that pure shear and *Vierendeel* bending are not critical, and combined global bending and shear at the load points should not reduce the bending resistance at the openings near the load points.

References

[1] Ahmed IM, Tsavdaridis KD. Life cycle assessment (LCA) and cost (LCC) studies of lightweight composite flooring systems. J Build Eng 2018;20:624–33.
[2] Ahmed IM, Tsavdaridis KD. The evolution of composite flooring systems: applications, testing, modelling and Eurocode design approaches. J Constr Steel Res 2019;155:286–300.
[3] Ahmed IM, Tsavdaridis KD. Shear connection of prefabricated slabs with lightweight concrete - Part 1: experimental and analytical work. J Constr Steel Res 2020;169.
[4] Ahmed IM, Tsavdaridis KD. Shear connection of prefabricated ultra-lightweight concrete slab system (PUSS_TM). Structures 2022;36:65–97.
[5] Alam N, Maraveas C, Tsavdaridis KD, Nadjai A. Performance of Ultra Shallow Floor Beams (USFB) Exposed to Standard Fires. J Build Eng 2021:102191.
[6] Brooks JJ, Bennett EW, Owens PL. Influence of lightweight aggregates on thermal strain capacity on concrete. Mag Concr Res 1987;39(139):60–72.
[7] BSI. Eurocode 4: Design of composite steel and concrete structures - Part 1-1: General rules and rules for buildings. London: BSI,; 2009.
[8] BSI. Eurocode 3: Design of steel structures – Part 1-1: General rules and rules of buildings. London: BSI,; 2015.
[9] BSI. Lightweight aggregates. London: BSI,; 2016.
[10] BSI. Testing hardened concrete - Part 3: Compressive strength of test specimens. London: BSI,; 2019.
[11] Chen S, Toi L, Tan J. Flexural behaviour of shallow cellular composite beams and innovative shear connections. J Constr Steel Res 2015;106:329–41.
[12] Huo BY, D'Mello CA. Push-out tests and analytical study of shear transfer mechanisms in composite shallow cellular floor beams. J Constr Steel Res 2013;88:191–205.
[13] Huo BY, D'Mello CA. Shear transferring mechanisms in a composite shallow cellular floor beam with web openings. Structures 2017;9:4–146.
[14] Kloeckner Metals U.K. (2017) Westok Ultra Shallow Floor Beam USFB™. Construction detail notes. ⟨https://www.kloecknermetalsuk.com⟩.
[15] Maraveas C, Tsavdaridis KD, Nadjai A. Fire resistance of partially unprotected ultra shallow floor beams (USFB): a numerical investigation. Fire Technol 2017;53(2):609–27.
[16] Pereira Junior SE, Ferreira FPV, Tsavdaridis KD, De Nardin S. Flexural behavior of steel-concrete ultra-shallow floor beams (USFBs) with precast hollow-core slab. Eng Struct 2023;278:115524.
[17] Sheehan T, Dai X, Tang J, Zhou K, Lam D. Flexural behaviour of composite slim floor beams. Structures 2019;21(1)):22–32.
[18] Slim floor beams preparation of application rules in view of improved safety, functionality and LCA (SlimApp), EU Report 30845 EN, 2021, Directorate General for Research and Innovation.
[19] Tsavdaridis, K.D. (2010) Structural Performance of Perforated Steel Beams with Novel Web Openings and with Partial Concrete Encasement. Doctoral Thesis, City University London, 2010. ⟨https://openaccess.city.ac.uk/id/eprint/11660/⟩.
[20] Tsavdaridis, K.D. and Giaralis, A. Derivation of Dynamic Properties of Steel Perforated Ultra Shallow Floor Beams (USFB) via Finite Element Modal Analysis and Experimental Verification. 7th Greek National Steel Structures Conference. 28 September – 1 October 2011, Volos, Greece, Reference no: 053, Vol. 2, pp. 321–329 ⟨http://eeme.ntua.gr/proceedings/7th/053.pdf⟩.
[21] Tsavdaridis KD, Giaralis A, Wang Z, Ferreira FPV. Vibration response of Ultra-Shalow Floor Beam (USFB) Composite Floors. Proceedings of the Institution of Civil Engineers - Structures and Buildings 2024. https://doi.org/10.1680/jstbu.23.00043.
[22] Wang J, Yang L, Shi Y, Zhang R. Loading capacity of composite slim frame beams. J Constr Steel Res 2009;65(3):650–61.